Human Molecular Genetics, 2018, Vol. 27, No. 11 1989–1998

doi: 10.1093/hmg/ddy106
Advance Access Publication Date: 23 March 2018
Original Article

ORIGINAL ARTICLE

Loss-of-function mutations in *FGF8* can be independent risk factors for holoprosencephaly

Sungkook Hong, Ping Hu, Erich Roessler, Tommy Hu and Maximilian Muenke*

Medical Genetics Branch, National Human Genome Research Institute, National Institutes of Health, Bethesda, MD 20892-3717, USA

*To whom correspondence should be addressed at: Medical Genetics Branch, National Human Genome Research Institute, National Institutes of Health, 35 Convent Drive, MSC 3717, Building 35, Room 1B-203, Bethesda, MD 20892-3717, USA. Tel: +1 3014028167; Fax: +1 3014967148; Email: mmuenke@nhgri.nih.gov

Abstract

The utilization of next generation sequencing has been shown to accelerate gene discovery in human disease. However, our confidence in the correct disease-associations of rare variants continues to depend on functional analysis. Here, we employ a sensitive assay of human *FGF8* variants in zebrafish to demonstrate that the spectrum of isoforms of FGF8 produced by alternative splicing can provide key insights into the genetic susceptibility to human malformations. In addition, we describe novel mutations in the FGF core structure that have both subtle and profound effects on ligand posttranslational processing and biological activity. Finally, we solve a case of apparent digenic inheritance of novel variants in *SHH* and *FGF8*, two genes known to functionally coregulate each other in the developing forebrain, as a simpler case of FGF8 diminished function.

Introduction

Holoprosencephaly (HPE) is anatomically distinguished from other midline malformations of the brain by the degree of separation of the eye field and telencephalon into discrete left and right structures. The phenotypic spectrum can range from mild craniofacial features, such as closely spaced eyes or solitary median central incisor, to the extreme of severe microcephaly, cyclopia and a proboscis (1). Molecularly similar and even identical mutations can be associated with either end of the phenotypic spectrum. *In utero*, HPE can be observed in 1:250 otherwise normal pregnancies but most affected fetuses fail to survive to term (2,3). HPE (due to mutations in *SHH*, *FGFR1*, *FGF8* and other genes) is presently considered distinct from disturbances of the hypothalamic–pituitary axis [Kallmann syndrome, idiopathic hypothalamic hypogonadism (IHH); *FGFR1, FGF8, HESX1, GLI2*, others], cleft lip and palate (CL/P) (*FGF8*, others), Culler–Jones syndrome (*GLI2*) and from septo-optic dysplasia (regulatory *SHH* variants, *HESX1*, others). However, we now appreciate that many of the causative genes and environmental teratogens are shared between these conditions (4–10). All of these conditions can demonstrate (1) similar prevalence rates in human populations; (2) incomplete penetrance; (3) variable expressivity and (4) have proponents for oligogenic or digenetic inheritance patterns (11,12); as well as (5) a suspected role for environmental modifiers (13,14). Interestingly, some of the very same mutations can be observed among probands classified with entirely different syndromes (4,15) (this study).

Detailed analysis of the murine locus for *Fgf8* defined a gene with a key role in body plan specification, tissue growth, differentiation, the epithelial/mesenchymal transition of epiblast cells that ingress into the primitive streak, the specification of the organizer and its axial mesendoderm derivatives, as well as participating in cooperative actions between several distinct patterning centers within the brain, face and limbs (16–23). Its coding region produces multiple isoforms through alternative splicing that encode proteins with distinct biological activities attributed to differential receptor binding affinity (23–27). The

Received: December 12, 2017. **Revised:** February 16, 2018. **Accepted:** March 19, 2018

most potent of these isoforms, Fgf8b, is indispensable for early development of the mouse and cannot be compensated for by the expression of either other FGF ligands or alternative Fgf8 isoforms (27–29). Furthermore, progressively severe phenotypes can be observed in mice with decreased levels of functional protein (30–32). Different tissue fields are impacted differently by such decreased signaling activity. For example, while both *FGFR1* and *FGF8* are strongly implicated in IHH pathogenesis, these patients rarely have limb anomalies. Although dominant negative mutations in *FGFR1* can perturb both tissues (33). Consequently, it is not hard to imagine that mutations at the human *FGF8* locus can lead to a spectrum of distinct phenotypic consequences due to the strength of the mutation and the actions of comorbid factors.

In humans, the first report of novel mutations in *FGF8* involved an isolated case of CL/P (34). Subsequently, mutations in either *FGFR1* or *FGF8* (occasionally both) were identified in human patients (IHH) with/or without anosmia (Kallmann syndrome, which is a form of IHH with absent sense of smell) (4,35–38). Experimental studies in mice confirm a role for both genes in the specification of the gonadotropin-releasing hormone secreting neurons in the hypothalamus and the development of the optic chiasm (39) and olfactory bulb (40). Although a potential role for FGF8 variants in HPE has been previously suggested (41), the detected variation had only minor functional disturbances, was also seen among IHH patients (35) and subsequently also among healthy controls (ExAC).

In this study, we set out to establish the role of FGF signaling in the pathogenesis of HPE using assays first developed in our analysis of Hartsfield syndrome (33,42,43). Recent studies have claimed a major role for FGF signaling in HPE, although functional studies were not provided to support their claims (15,36). Therefore, from a set of 330 HPE probands evaluated using a targeted capture panel of 150 developmental genes we selected 14 variants for further bioinformatics and functional analysis: two INDEL (one as a published positive control) (33), three novel putative splicing variants, one new autosomal recessive variant, one published autosomal recessive variant (36), two control SNPs seen in healthy individuals and five rare missense variants (Table 1; Roessler *et al.*, manuscript in preparation). Here, we show that the application of functional testing brings considerable clarity to the genotype/phenotype analysis and affirms many of the original pathogenetic assertions.

Results

Alternative splicing of human *FGF8* affects its biological activity

The exonic structure and genomic organization of the *Fgf8* gene is highly similar from teleosts to mammals, with the most important differences being limited primarily to variable exon usage at the amino-terminus (Supplementary Material, Table S1). In higher vertebrates, e.g. mouse and human, there is a variably utilized exon 1c that is absent in the most commonly tested isoforms (Fgfa and Fgfb) and the genomes of chick, frogs and zebrafish. This variable exon 1c is the site of numerous variants of unknown significance (Table 1). The physiological function of the first two exons (1a and 1b) is to encode the signal peptide that is required for efficient secretion of the signaling molecule. In mice, there is also an extended version of exon 1b that allows for the expression of eight isoforms through alternative splicing. In humans, there is a stop codon in this extended murine version of exon 1b that reduces the number of isoforms to only four (FGFa, FGF8b, FGF8e and FGF8f) (Supplementary Material, Fig. S1). For the purpose of mutation screening, we looked for variants in all six coding exons (1a, 1b, 1c, 1d[long] that completely overlaps exon 1d[short], exon 2 and exon 3).

Various experimental assays have previously established that the variable usage of alternative exon 1d splice acceptor sites can dramatically change the biological activity of Fgf8 isoforms, both *in vitro* and *in vivo* (29). As shown in Figure 1, this difference is also detected when we express the two longest human *FGF8* isoforms (e versus f) in zebrafish. For the purpose of determining the relative biological response of FGF8 protein variants (Table 1), we used the core structure of FGF8e (encoding exon 1c and 1d[short]). Our variant numbering reflects this choice as the wild-type (wt) isoform (NM_033164.3). The RNA injection-induced extreme toxicity (dorsalization and dead embryos) of the *FGFf* form effectively precluded its use as an efficient assay system in this study. This more potent f isoform was toxic at all doses tested. In contrast, using the *FGF8e* form showed a more moderate toxicity as a function of increasing RNA dose. Since we wanted to maximize our ability to measure less than wt biological activity differences, we selected the *FGF8e* cDNA backbone for site-directed mutagenesis. In doing so, we can show that using a 0.4 pg of *FGF8e* mRNA dose allowed us to measure a broader range of variant activity by measuring both a ratio of dorsalization/dead (50%) in our phenotypic scoring (see all doses tested) and also when compared with the use of 0.2 or 0.3 pg of the *FGF8f* isoform (Fig. 1B). Since the gene organization (and sequence context of the splice sites) is identical between murine *Fgf8* and human *FGF8*, we used bioinformatics analysis to interpret the consequences of mutations within or adjacent to the 1d[long] splice acceptor site (Supplementary Material, Table S1). As shown in Figure 1A (and described in Table 1), the utilization of the 1d[short] alternative acceptor site (resulting in the *FGF8e* isoform) reduces the effective biological response in humans as well as mice. Targeted removal of the 1d[long] acceptor site (eliminating the possibility for producing either *FGF8b* or *FGF8f*) in genetically modified mice is phenotypically identical to a $Fgf8^{null}$ allele and indicates that some biological functions of FGF8b (or FGF8f) cannot be compensated for by the actions of other ligands or isoforms (27,28).

FGF8 mutational findings in HPE patients

The human *FGF8* gene is relatively intolerant to sequence variation (pLI = 0.93; ExAC). No stop codon, frameshift, splice site or gene deletions among healthy individuals are currently described. Variations in exons 1a and 1c have been previously reported in humans; however, functional assays have not always been used to establish a direct connection with the observed phenotypes. Some variants were detected with equal or similar frequency in control populations (12,35,44) (Supplementary Material, Table S1) (33). Among HPE patients this variable exon 1c is also a common location of sequence variation (Table 1). The p.R28S, p.P30_A31insSAGPLP and p.R44W variants are all indistinguishable from wt in our functional assay system suggesting that their presence (or absence) in any of the isoforms contributes little to the biological effects (Fig. 2).

Among our HPE patients, we identified two novel sequential basepair variants in the invariant −1 position of acceptor site 1d[long] and the adjacent +1 position of the first codon (p.V53L) of 1d[long]. This clustering is remarkable given that no splice site variants are described among the 60 000 healthy controls in ExAC databases. Furthermore, four independent splicing analysis tools (Supplementary Material, Table S1) support the

Table 1. Clinical and molecular findings of genetic variants of the human *FGF8* gene

Patient	Variation[a]	Exon	Comment	Additional findings	MAF (ExAC)	Clinical[b]
BL9898	p.R28C	1c	Variable exon[c] (see also p.R28W among healthy controls; caution, poor read coverage)	Benign, confirmed by functional studies[d] N/A; benign, not tested	(0.0005410) absent; 8 findings in Kaviar	SCI, NPAS, E detected in controls
BL9631[e]	p.P30_A31 insSAGPLP	1c	Variable exon[c] (caution, poor read coverage)	None[d]	Absent	C, A, P, E
BL11445	p.R44W	1c	Variable exon[c] (caution, poor read coverage)	None[d]	0.0004287	RES, HyC, DD
BL9014	Splice acceptor [−1G>A][f]	1d[long]	Consistent usage accounts for increased potency[a]	None[d]	Absent	MIHV, CP, Hyp, Sz, E
BL7929	Near splice acceptor, p.V53L[f]	First base of 1d[long]	Accounts for increased potency[a]	None[d]	Absent	MIHV, CL/P, Mac, Sz
Guillen11955	p.E56Q	1d[short]	Negative control	None[d]	Absent	Unrelated healthy controls
BL9037	p.T108M	2	Second case of SL HPE (see text)	Normal Chr, (*SHH* p.S156R[d])	Absent (Absent)	SL, M, FFL, FBG, DD
BL11322	p.T122M	2	Homozygous, (consanguinity)	None[d]	Absent	SL, M, Hyp, Sz, DD
BL2216	Splice donor, IVS2 + 1[G>A][f]	2–3	Active in all isoforms	None[g]	Absent	No info.
rs139565972	p.V146I	3	Healthy controls (rs139565972)	N/A	0.00007441	N/A
BL11576	p.V146F	3	Receptor binding domain	Normal Chr, MicroA None[d]	Absent	SL, M, Sz, DD
BRZ8506	p.N155S	3	Receptor binding domain	None[g]	0.000008258	No info.
BL11058 and BL11059	c.515-529 delCCCGCAAGGGCCGGC	3	Confirmed as digenic	*FGFR1*[h]	Absent	SL, M, DD
Anonymous	p.R178H	3	Homozygous, (consanguinity)	None[i]	Absent	SL, DD, DI, PI

[a]Isoform e (NM_033164.3) (NP_149354.1) differs by 11 amino acids from the longest coding region isoform f by using an alternative (exon1d[long]) splice acceptor 33 bp upstream of exon1d[short]. These 11 amino acids provide and additional receptor contact site accounting for the increased potency of isoforms f > e and b > a. This alterative splicing (alternative potency of isoforms) is observed in all species from mammals to teleosts.

[b]SL, semilobar; M, microcephaly; NPAS, nasal pyriform aperture stenosis; E, ear anomalies; C, cyclopia; A, alobar; P, proboscis; RES, rhomboencephalosynapsis; HyC, hypoplastic single lobed cerebellum; DD, developmental delay; MIHV, middle interhemispheric variant; CP, cleft palate; CL/P, cleft lip and palate; Hyp, hypotelorism; Sz, seizures; Mac, macrocephaly; FFL, fusion of frontal lobes; FBG, fusion of basal ganglia; DI, diabetes insipidus; PI, pituitary insufficiency [ACTH and emergent TH and prolactin deficiency; see description (36)]; Chr, normal chromosomes; MicroA, normal microarray.

[c]Absent in isoforms *FGFa*, *FGFb*; not present in the genomes of chick, frogs or teleosts. Note that variants in this exon may not be physiologically important (44).

[d]CLIA testing was negative for deleterious variants in *SHH*, *ZIC2*, *SIX3* or *TGIF1* (except as noted). All variants in *FGF8* detected by targeted capture were also detected in exome data.

[e]Inherited from a healthy parent. Also seen in two unrelated families with parental data for analysis (BL6754 and BL4795).

[f]Splicing analysis (four independent methods) shown in Supplementary Material, Table S1.

[g]Predated CLIA lab. Targeted capture result. Confirmed by exome.

[h]Sibs with SL HPE and digenic inheritance (33).

[i]Described in (36).

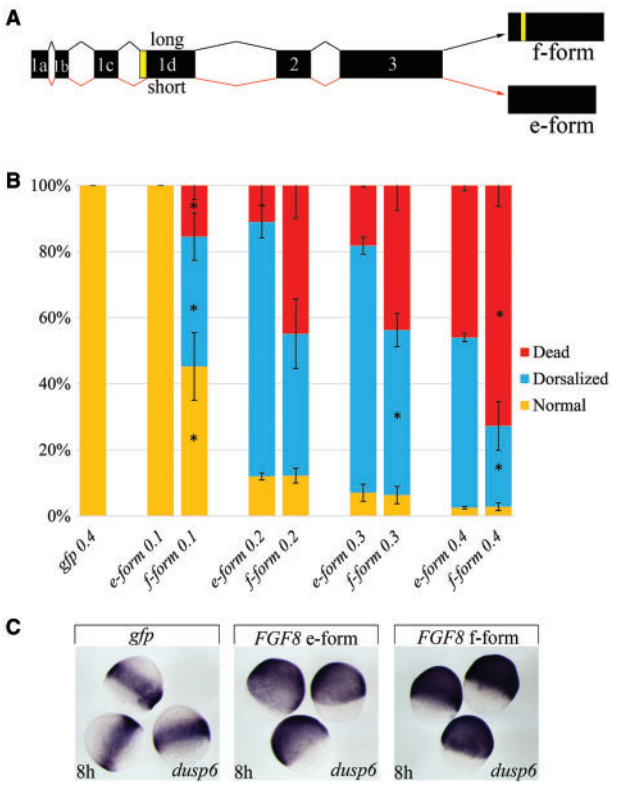

Figure 1. Alternative splice forms *FGF8e* and *FGF8f*. (**A**) The schematic genomic organization of the *FGF8* locus (exons not drawn to scale). The locus includes six exons that can be alternatively spliced to form four isoforms (*FGF8 a*, *b*, *e* and *f*). The two longest isoforms (e and f) differ by the alternative use of splice acceptor sites located 33 bp apart in the 5′ region of exon 1d. The 11 codons (indicated in yellow) account for a key additional contact residue that leads to differential binding to FGFR receptors. Variable use of exon 1c (not shown) accounts for two additional isoforms (*FGF8a* and *FGF8b*). (**B**) Biological response of FGF8e versus FGF8f. The biological response has been measured by injecting increasing amounts of synthetic *FGF8* mRNA of both forms in separate experiments and monitoring the phenotypic severity by scoring clutches of embryos. Note the dose–response is non-linear. The *FGF8e* form was the most sensitive to small changes in mRNA dose. A normal phenotype is shown in yellow, blue is for dorsalized embryos and red is for dead embryos. For each tested dose, the phenotypic responses are compared between the two isoforms in all three categories (yellow, blue and red). Error bars represent SEM. An asterix is used (*) to indicated that a given category (denoted by color) reaches a minimal level of significance ($P < 0.05$) between the two isoforms tested at the same dose. (**C**) A group image of *dusp6* gene expression as a biomarker sensitive to *FGF8* dose. Representative comparisons are shown between *FGF8e* and *FGF8f* followed by whole mount *in situ* hybridization at 8 h after fertilization. Quantification data in this study are described in Supplementary Material, Table S2.

skipping of this acceptor site (f isoform) for its downstream alternative (e isoform). Therefore, we infer that these sequence changes are equivalent to those artificially created in murine knock-in models and impose a haploinsufficiency on these probands for FGF8b activity. Similarly, the invariant splice donor site for IVS2+1[G>A] is predicted to affect all four *FGF8* isoforms and is also likely a loss-of-function allele. Any aberrant splicing between exons 2 and 3 inevitably alters the structure of the core receptor binding domain and heparin binding domain CDD: 238015.

As a negative control, we tested the p.E56Q variant that was novel but detected in a healthy individual without HPE. The overexpression of this variant in zebrafish is equivalent to the phenotypic and marker induction effects of the wt form (Fig. 2C and D). In contrast, the p.T108M variant was a complete loss-of-function allele with no dorsalizing activity, no marker induction properties, despite normal protein expression (compare Fig. 2C–E). The effects of the SHH p.S156R variant are described later (Fig. 4). Interestingly, the same molecular alteration has recently been described in a patient with semilobar HPE and a comorbid obligate deleterious splicing variant in *FGFR1* (15). Furthermore, the identical *FGFR1* splicing variant was first described in a patient with Kallmann syndrome which tends to blur the distinctions between these apparently unrelated conditions (4).

Autosomal recessive HPE is uncommon

Consanguinity is uncommon in our patient population but when present clearly has been described to predispose probands to autosomal recessive gene combinations (45). In our subject cohort, we observed a single case of homozygosity of a novel variant in the core receptor binding domain of FGF8. This p.T122M variant was assessed in our functional assay and determined to be a hypomorph and is, to our knowledge, the first experimentally confirmed case of homozygous recessive inheritance of FGF8 variants in HPE (Fig. 2C). Therefore, caution should be used to interpret novel variants in the homozygous state unless strong evidence of consistent transmission within a pedigree or the results of functional analysis are also considered (46,47). However, we can now provide support for a second instance of autosomal recessive inheritance of a *FGF8* variant (36), p.R178H, in HPE by using our functional assay to illustrate its utility (Fig. 2).

Different amino acid substitutions within a codon can have distinct effects

At the amino acid position p.V146 within the receptor binding core domain of FGF8 healthy individuals can have a rare substitution of isoleucine for valine. Such a variation is predicted by biochemistry and bioinformatics to be benign and indeed functional analysis confirms this prediction. However, substitution with a phenylalanine residue at this same position dramatically reduces the biological response of the mutant form (Fig. 2C). Although we suspect that this is due to altered receptor binding between the mutant form and its receptor partner, binding studies have not yet been performed. Interestingly, this patient has semilobar HPE and a genetic workup revealed normal chromosomes, normal microarray, normal four gene screen analysis (Table 1) and no comorbid variants in the targeted capture panel (data not shown).

Sequence variants can perturb glycosylation and inhibit biological activity

We have previously demonstrated that in-frame deletions within the heparin binding domain can interfere with FGF8 function (variant c.515–529delCCCGCAAGGGCCGGC in Table 1, Fig. 1, described in 33). This variant confirms that Fgf ligands can use heparin sulfate glycoproteins as coreceptors in physiological interactions. We now show that glycosylation of the FGF8 ligand itself can influence bioactivity. The p.N155S variant was identified in an anonymized Brazilian cohort of HPE patients added to our analysis to boost statistical power (Roessler *et al.*, manuscript in preparation). This variant is also seen once in ExAC databases. We noticed that the variant

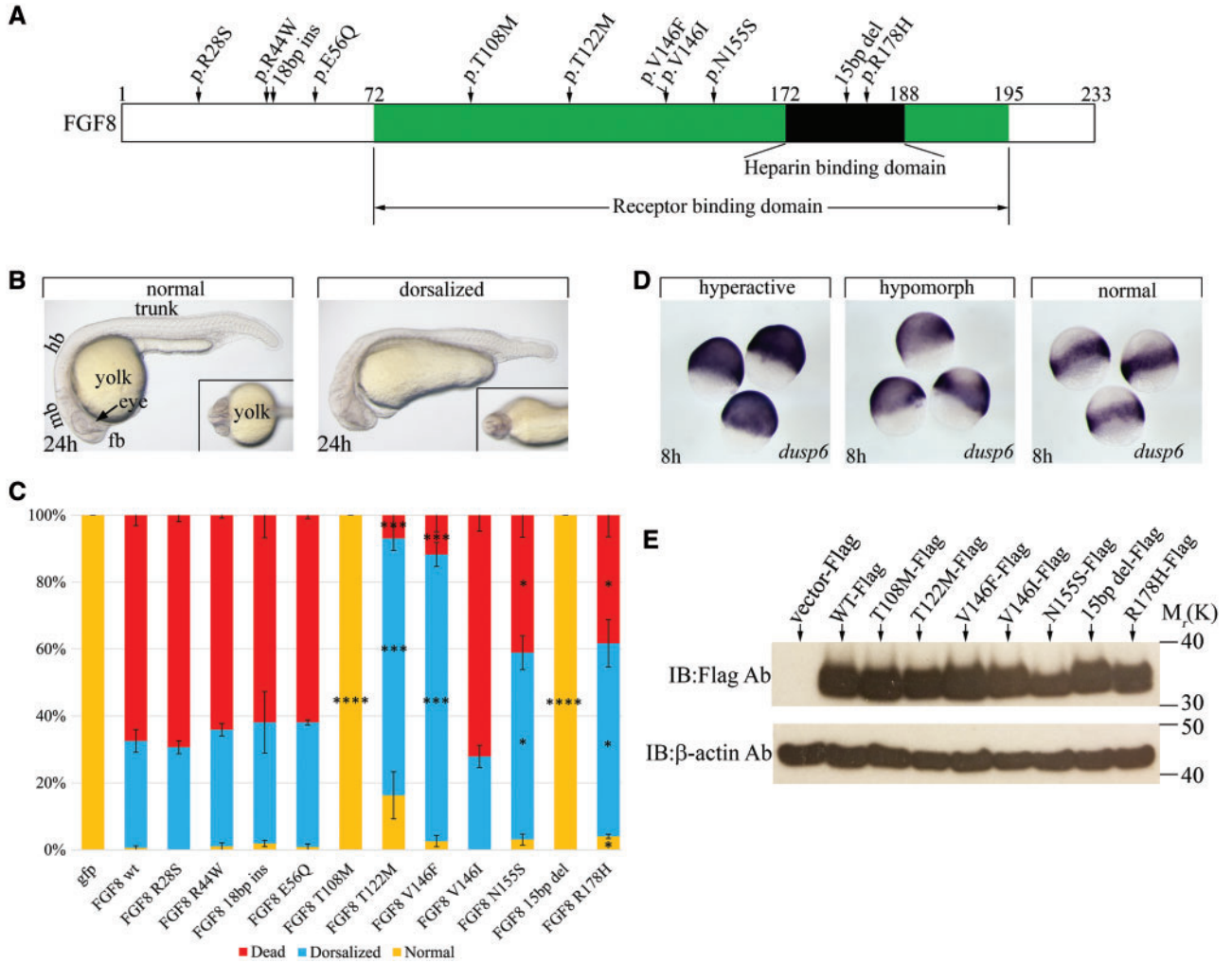

Figure 2. Functional analysis of *FGF8* variants in zebrafish. (**A**) Schematic representative of amino acid positions of variants and controls as measured by site-directed changes on the *FGF8e* isoform backbone (see proper names in Table 1). FGF receptor binding domain (green) and heparin binding domain (black) represent the FGF core structural elements common to all ligands in the FGF family (CDD: 238015). (**B**) Representative illustration of the *FGF8e* overexpression phenotypes at 24 hpf in zebrafish. Two clear phenotypic classes of embryos are observed in lateral (full image) and ventral view (inset image). The yellow color represents normal embryos and red is for dorsalized. (**C**) Results of *FGF8* mRNA injection. A 0.4 pg of *FGF8e* mRNA has been introduced into fertilized one-cell stage embryos and their biological response was measured by visual scoring of their phenotype at 24 hpf. The yellow color represents normal, red is for dead and blue for dorsalized by RNA injection. Normal phenotype was only observed in *FGF8 T108M* and *FGF8 15bp del*, which is consistent with a complete loss of function. Compared with *FGF8 wt*, *FGF8 T122M*, *FGF8 V146F*, *FGF8 N155S* and *FGF8 R178H* all present with a hypomorphic response. Error bars represent SEM, * indicates $P < 0.05$, *** indicates $P < 0.001$ and **** indicates $P < 10^{-8}$ when compared with *FGF8 wt* based on Student *t*-test. When appropriate, each category (by color) was independently compared with the expectation based on the *wt* response and given a statistical result. (**D**) Whole mount *in situ* hybridization of *dusp6* at 8 h. *wt FGF8e* is expected to produce a hyperactive induction of *dusp6* (FGF8e wt, 18bp ins, p.R44W, p.E56Q, p.V146I). Complete loss-of-function alleles are expected to stain normally (right panel; *gfp* control, *FGF8e p.T108M* and *FGF8e 15bp del*) while hypomorphic activity is somewhere between these extremes (middle panel; *FGF8e V146F*, *N155S*, *R178H*). (**E**) Western blot of FGF8 variants within the receptor binding domain region that demonstrate variable bioactivity. All constructs were tagged with Flag and transfected into Cos7 cell line and β-actin was used as loading control. Note that p.N155S migrates slightly faster (Fig. 3). Quantification data in this study are described in Supplementary Material, Table S2.

occurs within a consensus N-glycosylation site (N—any amino acid—S/T). Synthetic constructs were made for the observed mutation p.N155S, an alternative substitution p.N155I and a control variant p.T157A. All three variants eliminate the consensus glycosylation site and alter the migration of the post-translational protein products in transfected Cos7 and HEK293 cells (Fig. 3A and C). The wt Flag-tagged FGF8e, with an intact glycosylation site, is observed as a dimer on western blots of transfected cell lines. The slower migrating band is sensitive to PNGase F or endo H enzymatic cleavage (Fig. 3B). This result confirms that the genetic modification at positions p.155 and p.157 are indeed interfering with glycosylation *in vivo*. Interestingly, several sequence variations within this glycosylation site affect the bioactivity of the FGF8 molecule (Fig. 3D). The phenotypic effects of the p.N155S variant are yet to be fully documented.

Detection of comorbid variants does not prove oligogenic or digenic models

Although defective hedgehog signaling was nearly simultaneously discovered to cause HPE, first as cyclopia in the mouse (48) and then HPE in humans (49,50) there have been relatively few studies to determine the functional effects of various mutations (51). The hedgehog gene encodes two critical parts: the signaling functions are entirely due to the highly conserved

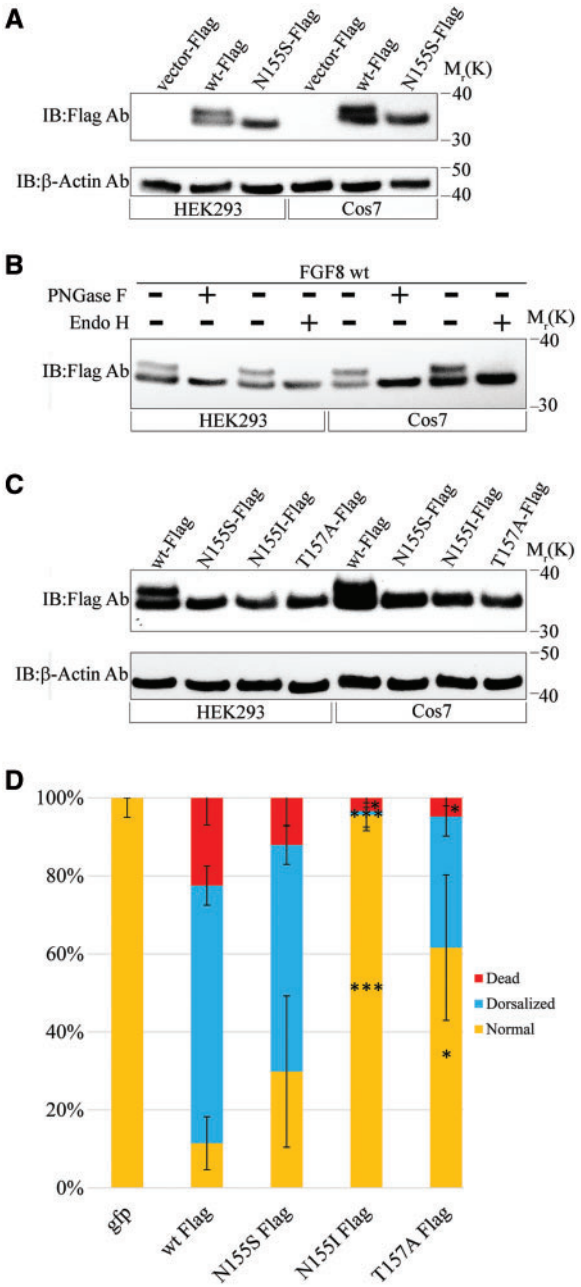

Figure 3. N-glycosylation analysis of the p.N155S variant. (**A**) Western blot results after transfection of FGF8e WT and FGF8e p.N155S into HEK293 and Cos7 cell lines. Note that the wt FGF8e migrates as a doublet. The variant p.N155S migrates a single faster migrating band. Flag ab was used for FGF8e detection and β-actin for lysate input control. (**B**) N-glycosylation test by PNGase F and Endo H enzyme treatment using the control FGF8e wt protein. Western performed after 1 h incubation of FGF8e wt protein with or without enzyme. (**C**) Western blot of the variant p.N155S, a synthetically made p.N155I, and p.T157A as controls. Note that the wt FGF8e migrates as a doublet and all variants affecting the consensus N-glycosylation site (N—any amino acid—S/T) migrate instead as a single band. This faster migrating band is identical to the product of PNGase or Endo H treatment. Confocal analysis of transfected Cos7 cells revealed no clear immunostaining differences between the Flag-tagged wt or variant forms (data not shown). (**D**) Injection of *N155S*, *N155I* and *T157A* mutants and phenotype analysis. Embryos were observed at 24 hpf and scored by their phenotype. Results for *N155S* ranged from normal to hypomorphic. Compared with *FGF8e wt flag* RNA injection, the synthetic constructs *N155I flag* and *T157A flag* exhibit loss of function. Results for p.N155S ranged from normal to hypomorphic in a series of five different experiments. The synthetic constructs p.N155I and p.T157A scored as loss-of-function in contemporaneous experiments. We conclude that glycosylation has subtle effects on bioactivity that can be profound in certain circumstances. Error bars represent SEM, * indicates $P < 0.05$ and ** indicates $P < 0.01$ when compared with *FGF8e* wt Flag based on Student *t*-test. Quantification data in this study are described in Supplementary Material, Table S2.

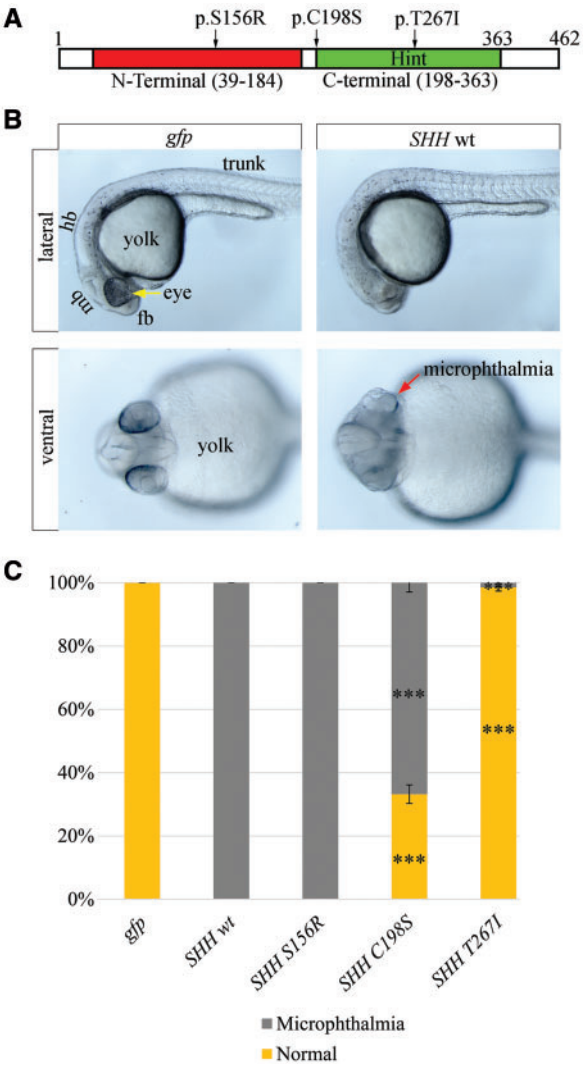

Figure 4. The comorbid *SHH* p.S156R missense variant (Table 1, seen with the loss-of-function FGF8 p.T108M) is functionally normal in zebrafish. (**A**) Schematic drawing of SHH functional domains [SHH-N, signaling domain (red); SHH-C, autoprocessing domain (green)] and the location of tested variant positions. The previously described cholesterol addition site mutation p.C198S and p.T267I were selected as hypomorphic and severe loss-of-function positive controls, respectively (60). (**B**) Lateral and ventral view of a representative 10 pg of *SHH* mRNA-injected embryo at 28 hpf (right panels). The yellow arrow points to the appearance of a normal sized zebrafish eye (gfp injection control), while the red arrow indicates a small eye (microphthalmia, right panels). (**C**) Quantitative measurements of control (*gfp*), *wt* and variants *SHH*-injected embryos. Yellow represents embryos with a normal phenotype and gray is for small eye (microphthalmia) embryos. Error bars represent SEM, *** indicates $P < 0.001$ when compared with *SHH* wt based on Student *t*-test. Quantification data in this study are described in Supplementary Material, Table S2.

amino-terminal domain that is dually lipidated by palmitate (52) and cholesterol, with the latter being an autocatalytic addition by the carboxy-terminal Hint motif (Fig. 4A) (53,54). Most mutations seen in the signaling domain are novel and often

meet the criteria for pathogenicity without the support of functional studies. Here, we illustrate the need for caution in these interpretations.

Patient BL9037 (Table 1) has inherited a novel complete loss-of-function mutation in *FGF8* (p.T108M) from one parent and a novel suspected loss-of-function mutation in *SHH* (p.S156R) from the other parent. At first glance, this appears to be a clear case of digenic inheritance. The p.T108M has been previously implicated in HPE (15) and proven to abnormal in our functional assays (see earlier). The comorbid *SHH* variant is also novel and occurs at a surface residue that experimentally is associated with binding to the tumor repressor *PTCH1* (55–58). Binding to PTCH1 is a prerequisite for hedgehog pathway activation (59). Furthermore, Fgf8 signals from the rostral signaling center are required to maintain the ventral signaling center responsible for eye field and telencephalic separation (principally hedgehog signals, see earlier) (31,32).

To determine the potential effects of variants in *SHH*, we performed an overexpression assay in zebrafish. At 28 h, zebrafish injected with the wt *SHH* full-length cDNA construct produces visibly reduced eyes (Fig. 4B) that can be scored and counted as a consistent bioassay measurement (Fig. 4C). In zebrafish, *shh* RNA injection causing a small eye phenotype has been previously described (60,61). As controls, we chose a point mutation at the site of cholesterol addition (p.C198S; known hypomorph) and the carboxy-terminal loss-of-function variant (p.T267I; both controls documented in 62). Under our assay conditions, the p.S156R variant is clearly normal. The control constructs closely resemble the hypomorphic and loss-of-function phenotypes previously published.

Discussion

The hedgehog signals (among others) necessary for the separation of the eye field and forebrain must act at the correct midline position, in the correct amount and at the correct time to correlate with normal development. The best understood causes of HPE affect one or more of these requirements. Rostral FGF signaling now emerges as a prerequisite for this midline signaling program. These functions are in addition to its earlier roles during gastrulation and later roles in craniofacial structures, the gut and limbs. We now appreciate that there is a positive feedback loop with the ventral midline hedgehog activity that induces *NKX2.1*, promotes *FOXG1* expression and forebrain growth, FGF provides key inhibitory actions on the dorsal signaling center (BMP, WNTs) that oppose ventral specification and promote dorsal structures of the cortical hem. This sophisticated cross talk between signaling centers is extremely sensitive to gene dose and small changes can have conflicting or confounding consequences (31,32). Assuming the critical window of HPE sensitivity is passed successfully, the development of the optic tracts, the retina and pigment epithelium, olfactory bulbs, pituitary and craniofacial structures may yet be perturbed by defects in FGF function. Hence, the phenotypic spectrum of coding (or non-coding) variation at the *FGF8* locus can have consequences for the development of all of these structures.

In this study, we provide compelling evidence that abnormal *FGF8* function can contribute to HPE. In many of our cases, there are no obvious comorbid gene alterations that suggest the necessity of either oligogenic or digenic cooperativity. Nevertheless, it is important to keep an open mind while further cases are analyzed and reported. Continued examination using functional analysis will help to deemphasize variants of unknown significance (44) (this study). To our knowledge, only *FGFR1* mutations are commonly *de novo* (33,42,43). None of our FGF8 mutations are documented to be *de novo*, although most are novel. Spontaneously novel microdeletion of the *FGF8* locus causes a contiguous gene deletion syndrome that supports the association with HPE and CL/P (63). Similarly, while not yet tested in our assay, the p.D73H (NP_149353.1) associated with CL/P is likely damaging by structural arguments and is also *de novo* (34).

Perhaps the most interesting observation from our study is that, although exceedingly uncommon, the same molecular variations are reported in diverse midline malformation syndromes. This is true for a complete loss-of-function in *FGF8* (p.T108M) in two unrelated patients with semilobar HPE. One had a second mutation in *FGFR1* that was absent in our patient (15) but previously described in Kallmann syndrome (4). In this report, a p.P129* stop codon mutation was described in a patient with HPE. Interestingly, this same alteration has previously been reported in IHH (64). The detection of the same variant in different contexts as inherited risk factors helps to support either reduced penetrance, variable expressivity or both. Oligogenic or digenic models are also not excluded and may help to explain these effects. The unmeasured role of environmental factors is an additional consideration that must be explored and validated. We maintain that comprehensive clinical examination, accurate phenotypic reporting, accurate sequencing with verification, combined with comprehensive data sharing will foster increased understanding and more accurate genetic counseling for our patients.

Materials and Methods

Patient samples and informed consent

All subjects provided informed consent for themselves and their affected children using approved forms and oversight from our NIH, NHGRI Institutional Review Board. Anonymous samples were obtained from our Brazilian colleagues by full-status collaboration, informed consent review and a total of 50 anonymous cases were added via an amendment to our larger Flagship study (Roessler *et al.*, manuscript in preparation). Institutional approval has been obtained for data sharing with investigators studying brain development and HPE. Medically relevant *FGF8* or *SHH* variants have been deposited into ClinVar.

Expression constructs

The *FGF8* cDNA, transcript variant e-form (NM_033164.3) has been described (29) and f-form (NM_033163.3) was purchased from (OriGene Technologies, Rockville, MD). All *FGF8* constructs were subcloned into the pCS2+ vector after PCR from cDNA resulting from clonal template purification. For western blot analysis, the indicated *FGF8* clones are tagged with Flag DNA sequences. The wt and mutant forms of *SHH* clones were also subcloned into a pCS2+ expression vector. The site-directed mutagenesis of *FGF8* and *SHH* performed according to instructions from company without modification (Agilent Technologies, Santa Clara, CA). All subcloned cDNA constructs were verified by Sanger sequencing.

Zebrafish husbandry

Wild-TAB5 strain was used in this study. The tropical zebrafish were maintained at 28°C according to: *The Zebrafish Book: A Guide for the Laboratory Use of Zebrafish (Danio rerio)*. All

experimental procedures have been approved and performed by following procedures described in our National Human Genome Research Institute animal protocol at the National Institutes of Health.

In vitro transcription and mRNA injection

The messenger RNA was generated using the mMESSAGE mMACHINE SP6 transcription kit (Thermo Fisher Scientific, Waltham, MA). A 0.4 pg bolus of *FGF8* synthetic mRNA was injected into fertilized one-cell stage embryos. To test the splicing effects on *FGF8*, 0.1–0.4 pg of *e-FGF8*, *f-FGF8* mRNA was introduced into embryos. A 10 pg bolus of *SHH* synthetic mRNA was injected to induce the small eye (microphthalmia) phenotype. All experimental tests of mRNA injections in this study were performed in triplicate and on different days. Quantification of embryos by phenotypic class can found in Supplementary Material, Table S2.

In situ hybridization

Antisense RNA probes were transcribed by SP6/T7 Transcription kit (Sigma-Aldrich, Saint Louis, MO). Whole mount *in situ* hybridization was performed as previously described (33) and were performed in triplicate. Molecular marker *dusp6* (33) was used as downstream biomarker of FGF signaling.

Transfection and immunoblot analysis

A total of 500 ng of Flag-tagged *FGF8* cDNA was transfected into HEK293 and Cos7 cell using a lipofectamine 2000 transfection reagent kit (Thermo Fisher Scientific) in 12-well tissue culture wells and the analysis has been done three times. After 24 h, cell lysis was performed with 200 μl of lysis buffer [20 mM Tris–HCl (pH 7.5) 150 mM NaCl, 1% TritonX-100] supplemented with a protease inhibitor cocktail (Thermo Fisher Scientific). For western blot analysis, 10% volume of lysate has been used for analysis. Primary antibody for this study was anti-Flag Mab (Sigma-Aldrich) and β-actin Mab (GeneTex, Irvine, CA) and secondary antibody was anti-rabbit IgG HRP (Cell Signaling, Danvers, MA) for Flag and anti-mouse IgG HRP (GeneTex) for β-actin antibody.

N-glycosylation assay

For the N-glycosylation test, Flag-tagged constructs were transfected into HEK293 and Cos7 cells. N-glycosylation assay has been done three times with both HEK293 and Cos7 cells. A 9 μl of whole lysate was used for analysis after lysis [20 mM Tris–HCl (pH.7.5) 150 mM NaCl, 1% TritonX-100] supplemented with protease inhibitor cocktail (Thermo Fisher Scientific). PNGase F and Endo H (New England Biolabs) enzyme methods were tested in this study by following the manufacture guidelines. Enzyme treatment was performed to full digestion during a 1 h incubation at 37°C.

Statistical analysis

All RNA injections are performed on different days and in three independent injections. For statistical analysis, experimental data was calculated with two-tailed Student *t*-test using Microsoft Excel 2010. Error bars on graphs are means (SEM).

Supplementary Material

Supplementary Material is available at *HMG* online.

Web Resources

Accession numbers and URLs for data presented herein are as follows
Online Mendelian Inheritance in Manh (OMIM), http://www.ncbi.nlm.nih.gov/Omim/
GeneBank, http://www.ncbi.nlm.nih.gov/GeneBank/
University of California Santa Cruz Bioinformatics Site, http://genome.ucsc.edu/
SplicePort, http://spliceport.cbcb.umd.edu/
MaxEntScan, http://genes.mit.edu/burgelab/maxent/Xmaxentscan_scoreseq.html
BDGP Berkeley Drosophila Genome Project, http://www.fruitfly.org/seq_tools/splice.html
NetGene2, http://www.cbs.dtu.dk/services/NetGene2/
1000 genomes browser, http://browser.1000genomes.org/index.html/
dbSNP, http://www.ncbi.nlm.nih.gov/projects/SNP/snp_ref.cgi/
Exome Variant Server, http://evs.gs.washington.edu/EVS/
Exome Aggregation Consortium, http://exac.broadinstitute.org/
All websites were last accessed on March 27, 2018.

Acknowledgements

The authors thank the patients and their families who participated in this research and the medical professionals that referred them.

Conflict of Interest statement. None declared.

Funding

This research was supported by the Division of Intramural Research (DIR), National Human Genome Research Institute, the National Institutes of Health.

References

1. Solomon, B.D., Mercier, S., Vélez, J.I., Pineda-Alvarez, D.E., Wyllie, A., Zhou, N., Dubourg, C., David, V., Odent, S., Roessler, E. *et al.* (2010) Analysis of genotype-phenotype correlations in human holoprosencephaly. *Am. J. Med. Genet.*, **154C**, 133–141.
2. Matsunaga, E. and Shiota, K. (1977) Holoprosencephaly in human embryos: epidemiologic studies of 150 cases. *Teratology*, **16**, 261–272.
3. Shiota, K. and Yamada, S. (2010) Early pathogenesis of holoprosencephaly. *Am. J. Med. Genet.*, **154C**, 22–28.
4. Dode, C., Levilliers, J., Dupont, J.M., De Paepe, A., Le Du, N., Soussi-Yanicostas, N., Coimbra, R.S., Delmaghani, S., Compain-Nouaille, S., Baverel, F. *et al.* (2003) Loss-of-function mutations in FGFR1 cause autosomal dominant Kallmann syndrome. *Nat. Genet.*, **33**, 463–465.
5. Roessler, E. and Muenke, M. (2010) The molecular genetics of holoprosencephaly. *Am. J. Med. Genet.*, **154C**, 52–61.
6. Raivio, T., Avbelj, M., McCabe, M.J., Romero, C.J., Dwyer, A.A., Tommiska, J., Sykiotis, G.P., Gregory, L.C., Diaczok, D., Tziaferi, V. *et al.* (2012) Genetic overlap in Kallmann syndrome, combined pituitary hormone deficiency, and septo-optic dysplasia. *J. Clin. Endocrinol. Metab.*, **97**, E694–E699.

7. Kietzman, H.W., Everson, J.L., Sulik, K.K. and Lipinski, R.J. (2014) The teratogenic effects of prenatal ethanol exposure are exacerbated by Sonic Hedgehog or GLI2 haploinsufficiency in the mouse. *PLoS One*, **9**, e89448.
8. Takagi, M., Takahashi, M., Ohtsu, Y., Sato, T., Narumi, S., Arakawa, H. and Hasegawa, T. (2016) A novel mutation in HESX1 causes combined pituitary hormone deficiency without septo optic dysplasia phenotypes. *Endocr. J.*, **63**, 405–410.
9. Hong, M. and Krauss, R.S. (2017) Ethanol itself is a holoprosencephaly-inducing teratogen. *PLoS One*, **12**, e0176440.
10. Kahn, B.M., Corman, T.S., Lovelace, K., Hong, M., Krauss, R.S. and Epstein, D.J. (2017) Prenatal ethanol exposure in mice phenocopies Cdon mutation by impeding Shh function in the etiology of optic nerve hypoplasia. *Dis. Model. Mech.*, **10**, 29–37.
11. Ming, J.E. and Muenke, M. (2002) Multiple hits during early embryonic development: digenic diseases and holoprosencephaly. *Am. J. Hum. Genet.*, **71**, 1017–1032.
12. Sykiotis, G.P., Plummer, L., Hughes, V.A., Au, M., Durrani, S., Nayak-Young, S., Dwyer, A.A., Quinton, R., Hall, J.E., Gusella, J.F. *et al.* (2010) Oligogenic basis of isolated gonadotropin-releasing hormone deficiency. *Proc. Natl. Acad. Sci. U. S. A.*, **107**, 15140–15144.
13. Krauss, R.S. and Hong, M. (2016) Gene-environment interactions and the etiology of birth defects. *Curr. Top. Dev. Biol.*, **116**, 569–580.
14. Hong, M., Srivastava, K., Kim, S., Allen, B.L., Leahy, D.J., Hu, P., Roessler, E., Krauss, R.S. and Muenke, M. (2017) BOC is a modifier gene in holoprosencephaly. *Hum. Mutat.*, **38**, 1464–1470.
15. Dubourg, C., Carre, W., Hamdi-Roze, H., Mouden, C., Roume, J., Abdelmajid, B., Amram, D., Baumann, C., Chassaing, N., Coubes, C. *et al.* (2016) Mutational spectrum in holoprosencephaly shows that FGF is a new major signaling pathway. *Hum. Mutat.*, **37**, 1329–1339.
16. Crossley, P.H. and Martin, G.R. (1995) The mouse Fgf8 gene encodes a family of polypeptides and is expressed in regions that direct outgrowth and patterning in the developing embryo. *Development*, **121**, 439–451.
17. Bueno, D., Skinner, J., Abud, H. and Heath, J.K. (1996) Spatial and temporal relationships between Shh, Fgf4, and Fgf8 gene expression at diverse signalling centers during mouse development. *Dev. Dyn.*, **207**, 291–299.
18. Harland, R. and Gerhart, J. (1997) Formation and function of Spemann's organizer. *Annu. Rev. Cell. Dev. Biol.*, **13**, 611–667.
19. Shimamura, K. and Rubenstein, J.L. (1997) Inductive interactions direct early regionalization of the mouse forebrain. *Development*, **124**, 2709–2718.
20. Sun, X., Meyers, E.N., Lewandoski, M. and Martin, G.R. (1999) Targeted disruption of Fgf8 causes failure of cell migration in the gastrulating mouse embryo. *Genes Dev.*, **13**, 1834–1846.
21. Crossley, P.H., Martinez, S., Ohkubo, Y. and Rubenstein, J.L. (2001) Coordinate expression of Fgf8, Otx2, Bmp4, and Shh in the rostral prosencephalon during development of the telencephalic and optic vesicles. *Neuroscience*, **108**, 183–206.
22. Ohkubo, Y., Chiang, C. and Rubenstein, J.L.R. (2002) Coordinate regulation and synergistic actions of BMP4, SHH and FGF8 in the rostral prosencephalon regulate morphogenesis of the telencephalic and optic vesicles. *Neuroscience*, **111**, 1–17.
23. Okada, T., Okumura, Y., Motoyama, J. and Ogawa, M. (2008) FGF8 signaling patterns the telencephalic midline by regulating putative key factors of midline development. *Dev. Biol.*, **320**, 92–101.
24. Gemel, J., Gorry, M., Ehrlich, G.D. and MacArthur, C.A. (1996) Structure and sequence of human FGF8. *Genomics*, **35**, 253–257.
25. Inoue, F., Nagayoshi, S., Ota, S., Islam, M.E., Tonou-Fujimori, N., Odaira, Y., Kawakami, K. and Yamasu, K. (2006) Genomic organization, alternative splicing, and multiple regulatory regions of the zebrafish fgf8 gene. *Dev. Growth Differ.*, **48**, 447–462.
26. Olsen, S.K., Li, J.Y., Bromleigh, C., Eliseenkova, A.V., Ibrahimi, O.A., Lao, Z., Zhang, F., Linhardt, R.J., Joyner, A.L. and Mohammadi, M. (2006) Structural basis by which alternative splicing modulates the organizer activity of FGF8 in the brain. *Genes Dev.*, **20**, 185–198.
27. Guo, Q. and Li, J.Y. (2007) Distinct functions of the major Fgf8 spliceform, Fgf8b, before and during mouse gastrulation. *Development*, **134**, 2251–2260.
28. Guo, Q., Li, K., Sunmonu, N.A. and Li, J.Y. (2010) Fgf8b-containing spliceforms, but not Fgf8a, are essential for Fgf8 function during development of the midbrain and cerebellum. *Dev. Biol.*, **338**, 183–192.
29. Sunmonu, N.A., Li, K. and Li, J.Y. (2011) Numerous isoforms of Fgf8 reflect its multiple roles in the developing brain. *J. Cell. Physiol.*, **226**, 1722–1726.
30. Meyers, E.N., Lewandoski, M. and Martin, G.R. (1998) An Fgf8 mutant allelic series generated by Cre- and Flp-mediated recombination. *Nat. Genet.*, **18**, 136–141.
31. Storm, E.E., Rubenstein, J.L. and Martin, G.R. (2003) Dosage of Fgf8 determines whether cell survival is positively or negatively regulated in the developing forebrain. *Proc. Natl. Acad. Sci. U. S. A.*, **100**, 1757–1762.
32. Storm, E.E., Garel, S., Borello, U., Hebert, J.M., Martinez, S., McConnell, S.K., Martin, G.R. and Rubenstein, J.L. (2006) Dose-dependent functions of Fgf8 in regulating telencephalic patterning centers. *Development*, **133**, 1831–1844.
33. Hong, S., Hu, P., Marino, J., Hufnagel, S.B., Hopkin, R.J., Toromanović, A., Richieri-Costa, A., Ribeiro-Bicudo, L.A., Kruszka, P., Roessler, E. *et al.* (2016) Dominant-negative kinase domain mutations in FGFR1can explain the clinical severity of Hartsfield syndrome. *Hum. Mol. Genet.*, **25**, 1912–1922.
34. Riley, B.M., Mansilla, M.A., Ma, J., Daack-Hirsch, S., Maher, B.S., Raffensperger, L.M., Russo, E.T., Vieira, A.R., Dode, C., Mohammadi, M. *et al.* (2007) Impaired FGF signaling contributes to cleft lip and palate. *Proc. Natl. Acad. Sci. U. S. A.*, **104**, 4512–4517.
35. Falardeau, J., Chung, W.C., Beenken, A., Raivio, T., Plummer, L., Sidis, Y., Jacobson-Dickman, E.E., Eliseenkova, A.V., Ma, J., Dwyer, A. *et al.* (2008) Decreased FGF8 signaling causes deficiency of gonadotropin-releasing hormone in humans and mice. *J. Clin. Invest.*, **118**, 2822–2831.
36. McCabe, M.J., Gaston-Massuet, C., Tziaferi, V., Gregory, L.C., Alatzoglou, K.S., Signore, M., Puelles, E., Gerrelli, D., Farooqi, I.S., Raza, J. *et al.* (2011) Novel FGF8 mutations associated with recessive holoprosencephaly, craniofacial defects, and hypothalamo-pituitary dysfunction. *J. Clin. Endocrinol. Metab.*, **96**, E1709–E1718.
37. Miraoui, H., Dwyer, A. and Pitteloud, N. (2011) Role of fibroblast growth factor (FGF) signaling in the neuroendocrine control of human reproduction. *Mol. Cell. Endocrinol.*, **346**, 37–43.
38. Miraoui, H., Dwyer, A.A., Sykiotis, G.P., Plummer, L., Chung, W., Feng, B., Beenken, A., Clarke, J., Pers, T.H., Dworzynski, P.

et al. (2013) Mutations in FGF17, IL17RD, DUSP6, SPRY4, and FLRT3 are identified in individuals with congenital hypogonadotropic hypogonadism. *Am. J. Hum. Genet.*, **92**, 725–743.
39. Chung, W.C., Moyle, S.S. and Tsai, P.S. (2008) Fibroblast growth factor 8 signaling through fibroblast growth factor receptor 1 is required for the emergence of gonadotropin-releasing hormone neurons. *Endocrinology*, **149**, 4997–5003.
40. Hu, Y., Poopalasundaram, S., Graham, A. and Bouloux, P.M. (2013) GnRH neuronal migration and olfactory bulb neurite outgrowth are dependent on FGF receptor 1 signaling, specifically via the PI3K p110alpha isoform in chick embryo. *Endocrinology*, **154**, 388–399.
41. Arauz, R.F., Solomon, B.D., Pineda-Alvarez, D.E., Gropman, A.L., Parsons, J.A., Roessler, E. and Muenke, M. (2010) A hypomorphic allele in the FGF8 gene contributes to holoprosencephaly and is allelic to gonadotropin-releasing hormone deficiency in humans. *Mol. Syndromol.*, **1**, 59–66.
42. Simonis, N., Migeotte, I., Lambert, N., Perazzolo, C., de Silva, D.C., Dimitrov, B., Heinrichs, C., Janssens, S., Kerr, B., Mortier, G. *et al*. (2013) FGFR1 mutations cause Hartsfield syndrome, the unique association of holoprosencephaly and ectrodactyly. *J. Med. Genet.*, **50**, 585–592.
43. Dhamija, R., Kirmani, S., Wang, X., Ferber, M.J., Wieben, E.D., Lazaridis, K.N. and Babovic-Vuksanovic, D. (2014) Novel de novo heterozygous FGFR1 mutation in two siblings with Hartsfield syndrome: a case of gonadal mosaicism. *Am. J. Med. Genet.*, **164**, 2356–2359.
44. Zeidler, C., Woelfle, J., Draaken, M., Mughal, S.S., Grosse, G., Hilger, A.C., Dworschak, G.C., Boemers, T.M., Jenetzky, E., Zwink, N. *et al*. (2014) Heterozygous FGF8 mutations in patients presenting cryptorchidism and multiple VATER/VACTERL features without limb anomalies. *Birth Defects Res. A Clin. Mol. Teratol.*, **100**, 750–759.
45. Mouden, C., de Tayrac, M., Dubourg, C., Rose, S., Carré, W., Hamdi-Rozé, H., Babron, M.-C., Akloul, L., Héron-Longe, B., Odent, S. *et al*. (2015) Homozygous STIL mutation causes holoprosencephaly and microcephaly in two siblings. *PLoS One*, **10**, e0117418.
46. Kumar, A., Girimaji, S.C., Duvvari, M.R. and Blanton, S.H. (2009) Mutations in STIL, encoding a pericentriolar and centrosomal protein, cause primary microcephaly. *Am. J. Hum. Genet.*, **84**, 286–290.
47. Kakar, N., Ahmad, J., Morris-Rosendahl, D.J., Altmuller, J., Friedrich, K., Barbi, G., Nurnberg, P., Kubisch, C., Dobyns, W.B. and Borck, G. (2015) STIL mutation causes autosomal recessive microcephalic lobar holoprosencephaly. *Hum. Genet.*, **134**, 45–51.
48. Chiang, C., Litingtung, Y., Lee, E., Young, K.E., Corden, J.L., Westphal, H. and Beachy, P.A. (1996) Cyclopia and defective axial patterning in mice lacking Sonic Hedgehog gene function. *Nature*, **383**, 407–413.
49. Roessler, E., Belloni, E., Gaudenz, K., Jay, P., Berta, P., Scherer, S.W., Tsui, L.C. and Muenke, M. (1996) Mutations in the human Sonic Hedgehog gene cause holoprosencephaly. *Nat. Genet.*, **14**, 357–360.
50. Belloni, E., Muenke, M., Roessler, E., Traverso, G., Siegel-Bartelt, J., Frumkin, A., Mitchell, H.F., Donis-Keller, H., Helms, C., Hing, A.V. *et al*. (1996) Identification of Sonic Hedgehog as a candidate gene responsible for holoprosencephaly. *Nat. Genet.*, **14**, 353–356.
51. Singh, S., Tokhunts, R., Baubet, V., Goetz, J.A., Huang, Z.J., Schilling, N.S., Black, K.E., MacKenzie, T.A., Dahmane, N. and Robbins, D.J. (2009) Sonic Hedgehog mutations identified in holoprosencephaly patients can act in a dominant negative manner. *Hum. Genet.*, **125**, 95–103.
52. Pepinsky, R.B., Zeng, C., Wen, D., Rayhorn, P., Baker, D.P., Williams, K.P., Bixler, S.A., Ambrose, C.M., Garber, E.A., Miatkowski, K. *et al*. (1998) Identification of a palmitic acid-modified form of human Sonic Hedgehog. *J. Biol. Chem.*, **273**, 14037–14045.
53. Cooper, M.K., Wassif, C.A., Krakowiak, P.A., Taipale, J., Gong, R., Kelley, R.I., Porter, F.D. and Beachy, P.A. (2003) A defective response to Hedgehog signaling in disorders of cholesterol biosynthesis. *Nat. Genet.*, **33**, 508–513.
54. Grover, V.K., Valadez, J.G., Bowman, A.B. and Cooper, M.K. (2011) Lipid modifications of Sonic Hedgehog ligand dictate cellular reception and signal response. *PLoS One*, **6**, e21353.
55. Goodrich, L.V., Milenkovic, L., Higgins, K.M. and Scott, M.P. (1997) Altered neural cell fates and medulloblastoma in mouse patched mutants. *Science*, **277**, 1109–1113.
56. Pepinsky, R.B., Rayhorn, P., Day, E.S., Dergay, A., Williams, K.P., Galdes, A., Taylor, F.R., Boriack-Sjodin, P.A. and Garber, E.A. (2000) Mapping Sonic Hedgehog-receptor interactions by steric interference. *J. Biol. Chem.*, **275**, 10995–11001.
57. Beachy, P.A., Hymowitz, S.G., Lazarus, R.A., Leahy, D.J. and Siebold, C. (2010) Interactions between Hedgehog proteins and their binding partners come into view. *Genes Dev.*, **24**, 2001–2012.
58. Tukachinsky, H., Petrov, K., Watanabe, M. and Salic, A. (2016) Mechanism of inhibition of the tumor suppressor patched by Sonic Hedgehog. *Proc. Natl. Acad. Sci. U. S. A.*, **113**, E5866–E5875.
59. Ingham, P.W., Nakano, Y. and Seger, C. (2011) Mechanisms and functions of Hedgehog signalling across the metazoa. *Nat. Rev. Genet.*, **12**, 393–406.
60. Krauss, S., Concordet, J.P. and Ingham, P.W. (1993) A functionally conserved homologue of the Drosophila segment polarity gene hh is expressed in tissues with polarizing activity in zebrafish embryos. *Cell*, **75**, 1431–1444.
61. Macdonald, R., Barth, K.A., Xu, Q., Holder, N., Mikkola, I. and Wilson, S.W. (1995) Midline signalling is required for Pax gene regulation and patterning of the eyes. *Development*, **121**, 3267–3278.
62. Tokhunts, R., Singh, S., Chu, T., D'Angelo, G., Baubet, V., Goetz, J.A., Huang, Z., Yuan, Z., Ascano, M., Zavros, Y. *et al*. (2010) The full-length unprocessed hedgehog protein is an active signaling molecule. *J. Biol. Chem.*, **285**, 2562–2568.
63. Peltekova, I.T., Hurteau-Millar, J. and Armour, C.M. (2014) Novel interstitial deletion of 10q24.3-25.1 associated with multiple congenital anomalies including lobar holoprosencephaly, cleft lip and palate, and hypoplastic kidneys. *Am. J. Med. Genet. A*, **164A**, 3132–3136.
64. Trarbach, E.B., Abreu, A.P., Silveira, L.F., Garmes, H.M., Baptista, M.T., Teles, M.G., Costa, E.M., Mohammadi, M., Pitteloud, N., Mendonca, B.B. *et al*. (2010) Nonsense mutations in FGF8 gene causing different degrees of human gonadotropin-releasing deficiency. *J. Clin. Endocrinol. Metab.*, **95**, 3491–3496.